Catalysis Science & Technology

Accepted Manuscript

ROYAL SOCIETY OF CHEMISTRY

www.rsc.org/catalysis

Journal Name

RSCPublishing

ARTICLE

Mechanistic Study and Catalyst Development of Selective Carbon Monoxide Methanation

Cite this: DOI: 10.1039/x0xx00000x

S. Tada,[a,b] and R. Kikuchi*[a]

Received ooth January 2012,
Accepted ooth January 2012

DOI: 10.1039/x0xx00000x

www.rsc.org/

Selective CO methanation has been attractive as a CO removal technique from reforming gases in polymer electrolyte fuel cell systems. The catalysts for the title reaction require the following two features: (i) high CO methanation activity at low temperatures and (ii) low CO_2 methanation activity at high temperatures. In this review, we surveyed numerous studies of selective CO methanation using heterogeneous catalysts, and discussed its plausible mechanism. Furthermore, we summarized how the activity and selectivity of CO methanation can be affected by particle size of active metal, support materials, and additives.

Introduction

Polymer electrolyte fuel cells (PEFCs) produce electric energy via the oxidation of hydrogen with high power density and conversion efficiency, and are expected to be in the practical applications such as the portable power source for electric vehicles, mobile phones, and so on. Especially Japan, South Korea, Germany, and the U. S. lead the world in the research and development of PEFC systems. [1] In Japan, for example, PEFC systems have been commercially available by the name of ENE-FARM since 2009, and it was expected that 50,000 units would be installed by the end of fiscal year 2013. The retail price of PEFC is gradually decreasing to 25,000 USD per kW, but remains expensive for domestic facilities. In order to spread PEFC systems, it is necessary to manufacture PEFC at a low cost and in large numbers. The following 4 topics have been studied all over the world for the significant cost reduction of the full-fledged commercialization of residential PEFC co-generation systems: a development of durable electrolyte materials, a development of CO tolerant anode catalysts, a development of CO removal processes from reformates, and a method to estimate the influence of impurities on fuel cell performance. As will be seen, this review focuses on the CO removal processes by selective CO methanation.

In the future hydrogen could be made from water electrolysis using renewable energy resources, while hydrogen is presently made mainly from fossil fuels. The schematic diagram of the fuel processing for conventional PEFC systems is shown in Fig. 1 (A). As one of the problem for the systems, the concentration of CO in the hydrogen-rich gas must be reduced to < 100 ppm before feeding the hydrogen-rich gas to the PEFC anode.[2] Otherwise a small amount of CO poisons the Pt catalysts on the anode. The CO concentration can be reduced from ca. 10 % to 0.2-2 % by the water gas shift reaction (WGS reaction, $CO + H_2O \rightarrow CO_2 + H_2$), and then to < 100 ppm by preferential oxidation of CO in the presence of excess H_2 (PROX, $CO + 1/2O_2 \rightarrow CO_2$). However, during PROX hydrogen is inevitably oxidized in the presence of oxygen, leading to a decrease in the PEFC energy conversion efficiency.

$$CO + 3H_2 \rightarrow CH_4 + H_2O \qquad \Delta H_{298}^{o} = -206 \text{ kJ mol}^{-1} \quad \text{(eq. 1)}$$

$$CO_2 + 4H_2 \rightarrow CH_4 + 2H_2O\ (g) \qquad \Delta H_{298}^{o} = -165 \text{ kJ mol}^{-1} \quad \text{(eq. 2)}$$

$$CO_2 + H_2 \rightarrow CO + H_2O\ (g) \qquad \Delta H_{298}^{o} = 41 \text{ kJ mol}^{-1} \quad \text{(eq. 3)}$$

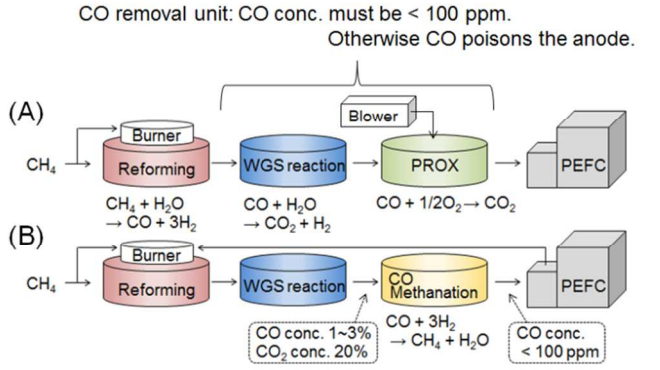

Fig. 1 Fuel processing for PEFC systems with a unit of (A) preferential oxidation of CO (PROX) and (B) CO methanation.

Another alternative is CO methanation (eq. 1) carried out in the presence of excess CO_2 (Fig. 1 (B)). Methanation of CO has the advantages that the reactants are already present for this reaction (CO and H_2) in the reformates, and that the produced

CH_4 can be recycled as a heating fuel for the reforming unit. High selectivity for CO methanation is important in the elimination of CO by methanation, otherwise simultaneous CO_2 methanation (eq. 2) and the reverse water-gas shift reaction (RWGS reaction, eq. 3) can give rise to extremely large consumption of produced H_2 as well as runaway of the methanation reactor due to the highly exothermic nature of the CO_2 methanation reaction. To obtain a wide operating temperature window for selective CO methanation, suitable catalysts must be developed that carry out CO methanation at low temperatures and do not favor CO_2 methanation and the RWGS reaction at high temperatures.

In the early stages of selective CO methanation study, a lot of researchers attempted to choose suitable active metals for selective CO methanation. Traditionally Ru, Rh, Ni, Co, and Fe catalysts have been used as industrial catalysts for CO and CO_2 methanation and Fischer-Tropsch synthesis. However, the metal catalysts with high activity of CO methanation normally promote undesirable CO_2 methanation. Therefore the choice is very important for those who study and design selective CO methanation catalysts. Panagiotopoulou et al. surveyed the performance of supported noble metal (Ru, Rh, Pt, and Pd) catalysts for selective CO methanation, and methanation activity of Ru and Rh catalysts was higher compared to Pt and Pd catalysts.[3] Takenaka et al. investigated the catalytic nature of active species (Ru, Co, Ni, Fe, Pd, and Pt) on SiO_2 as well. [4] Over Ru, Co, and Ni on SiO_2, CO was converted at the temperature below 380ºC, while over Fe, Pd, and Pt on SiO_2, CO remained unreacted. In spite of high CO conversion, Co species does not seem to be suitable active species because Co catalysts improve not only an activity of CO hydrogenation but also an activity of WGS reaction.[4-6] In consequence, recently a lot of researchers have studied Ru[3, 4, 7-25] and Ni [4, 5, 26-29] catalysts.

Three comprehensive reviews about CO removal processes from reformates, published in 2009, [30] 2011, [31] and 2013, [32] focused partly on selective CO methanation, and covered a few studies. Accordingly there is no review featuring only the title reaction. In this review, articles on selective CO methanation published mainly in this decade will be discussed. Initially, we will first discuss in section 2 the plausible mechanism of CO and CO_2 methanation under CO and CO_2 coexisting condition. After that, we will show the effect of particle size (section 3) and electron density (section 4) of active species on selective CO methanation. As will be shown in section 5, we will discuss the suppression of CO_2 adsorption or conversion to CO in the title reaction.

2. Mechanistic study of CO or CO_2 methanation

2.1 CO methanation

The reaction pathway of methanation of CO is often proposed. It is reported that CO methanation over supported metal catalysts proceeds via the dissociation of CO on the metal and the successive hydrogenation of the resultant surface carbonaceous species. [33-35] Methanation of CO under CO and CO_2 coexisting condition is also considered to take place at the active metal surface.[12, 16] Panagiotopoulou and coauthors precisely analysed the nature of Ru species on TiO_2 during CO and/or CO_2 methanation using in-situ DRIFT and TPD technique.[16, 17] Under CO methanation condition, the following CO species were observed: linear and bridged CO on metallic Ru (Ru_x-CO), multicarbonyl species on partially oxidized Ru ($Ru^{n+}(CO)_x$), and Ru-CO located at the metal-support interface ((TiO_2)Ru-CO). The presence of $Ru^{n+}(CO)_x$ may indicate the dissociative adsorption of CO.[14, 36] The authors concluded that hydrogenation of surface carbon produced by dissociative adsorption of CO on metal Ru (**eqs. 4-6**) was much faster than that of (TiO_2)Ru-CO, and the main route of CO methanation at low temperature (< 300 ºC).

$$CO + Ru_x \leftrightarrow Ru_x\text{-}CO \qquad \text{(eq. 4)}$$

$$Ru_x\text{-}CO + Ru \rightarrow Ru_x\text{-}C + Ru\text{-}O \qquad \text{(eq. 5)}$$

$$Ru_x\text{-}C + 4H(a) \rightarrow Ru_x + CH_4 \qquad \text{(eq. 6)}$$

2.2 CO_2 methanation

The mechanism of CO_2 methanation has been mainly investigated using Ni [29, 37-40] and noble metals (such as Ru,[41, 42] Rh,[43] and Pd [44]) as active species supported on various metal oxides. As for CO_2 methanation over supported metal catalysts, it is well accepted that CO_2 adsorbed on the catalyst surface reacts with H_2 on the metal to produce methane. However, there still exists argument that the active sites of the conversion from CO_2 to CO over supported catalysts are the metal surface [29, 37, 39, 40, 43] or interface between the metal and the support. [38, 41] In this section, we would like to show recent findings about CO_2 methanation mechanism with a focus on IR data.

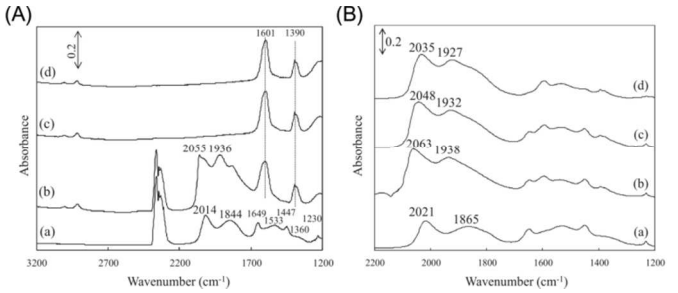

Fig. 2 (A) DRIFT spectra for CO_2 adsorption and hydrogenation over unmodified Ni–Al oxide catalyst added under flowing (a) CO_2, (b) CO_2 and H_2, (c) H_2 for 5 min, and (d) H_2 for 30 min. (B) DRIFT spectra for CO_2 and CO adsorption over unmodified Ni-Al oxide under flowing (a) CO_2, (b) CO_2+CO, (c) CO_2, (d) He. These measurements were carried out sequentially at 230°C. Reproduced from Ref. [45].

Miyao and coauthors examined CO_2 adsorption and hydrogenation over Ni-Al oxide using in-situ DRIFT, as illustrated in **Fig. 2** (A). [45] After dosing CO_2 to the chamber, the peaks attributed to CO adsorbed on metallic Ni appeared at 2014 and 1844 cm^{-1} (**Fig. 2** (A-a)). Furthermore H_2 was subsequently added to the CO_2 flow, and the peaks of CO grew

and the peaks of formate (1601 and 1390 cm^{-1}) and C-H vibration (ca. 3000 cm^{-1}) emerged (**Fig. 2** (A-b)). After switching CO_2/H_2 gas mixture to H_2, the CO peaks disappeared, and the peaks of formate and C-H vibration slightly decreased (**Fig. 2** (A-c, d)). Accordingly, they suggested that CO_2 was converted to CO not via the formate route (as mentioned below), but via the following steps: CO_2 adsorbed on Ni sites can be dissociated to Ni-CO and Ni-O, and additional CO via RWGS reaction adsorbed on the vacant Ni sites. Moreover they attempted to identify the predominant cites for CO_2 conversion to CO, and dosed CO on the CO_2-modified catalyst surface (**Fig. 2** (B)). Thereupon the peak area of adsorbed CO twofold increased (**Fig. 2** (B-a, b)). Next they stated that adsorbed CO species were almost unchanged after exchanging the gas mixture to CO_2, and subsequently to He (**Fig. 2** (B-c, d)).

We, however, considered that after switching the dosing gas from CO_2/CO mixture to CO_2 and then to He, the peaks of CO in Fig. 2 (B) were red shifted due to a decrease in CO surface coverage, in other words, CO desorption (Figs. 2(B) b-d). [46] It is expected that CO was not produced but desorbed from the catalyst in spite of CO_2 introduction to the chamber. Furthermore, the CO_2 dissociation did not oxidize the Ni surface; otherwise the peaks of Ni^+–CO would appear at ca. 2150 cm^{-1} in Fig. 2 (B-b).[47] These can indicate that the reaction sites of CO_2 conversion are almost different from the adsorption ones of CO. Several researchers proposed that CO_2 conversion to CO should take place at the metal-support interface because most of CO_2 adsorbs not on active metal but on support material.[9, 16, 17, 38, 41, 48-50]

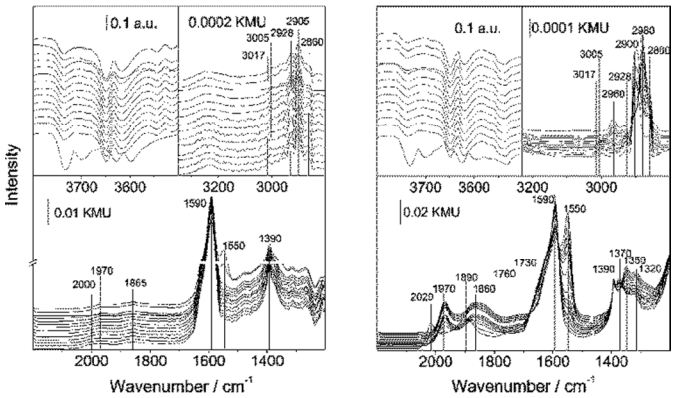

Fig. 3 DRIFT spectra recorded during 1000 min on stream at 190°C (equilibration of surface species) over the Ru/zeolite (left panels) and the Ru/Al_2O_3 catalysts (right panels) in CO_2-rich reformate and subsequent change to $^{13}CO_2$ containing reaction atmosphere: From bottom to top: 0, 1, 2, 3, 5, 6, 7, 10, 15, 20, 25, 30, 35, 45 min. Reproduced from Ref. [12].

In order to reveal the mechanism of CO_2 methanation, it is also quite necessary to consider what the intermediates of CO_2 methanation are. Eckel and coauthors employed steady-state isotope transient kinetic analysis (SSITKA) IR measurements, as shown in Fig. 3. [12] After 1000 min reaction test of CO_2 methanation over Ru/zeolite and Ru/Al_2O_3, the gas mixture ($^{12}CO_2/H_2$) switched to that including isotope labelled isotopomer ($^{13}CO_2/H_2$). Then ^{12}C-containing formate species (1590 cm^{-1}) somewhat disappeared, and ^{13}C-containing formate species (1550 cm^{-1}) gradually appeared. In addition, ^{12}C-containing species of CO (ca. 2000 cm^{-1}) and C-H vibration (ca. 3000 cm^{-1}) were also exchanged to ^{13}C-containig species. From these results they considered that the CO cannot be formed via formate species derived from RWGS reaction but CO_2 dissociation to CO. As mentioned above in Fig. 2 (A), Miyao and coauthors concluded that formate species is not an intermediate of CO_2 methanation under CO and CO_2 coexisting condition. Noteworthily, both studies ignored bare disappearance of formate species.

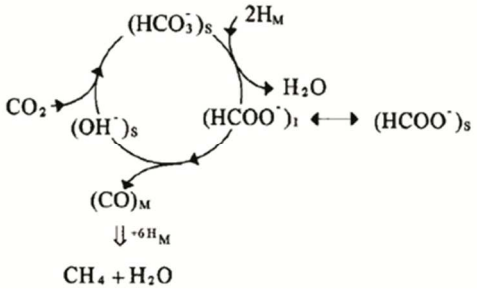

Scheme 1 CO_2 methanation over Ru/TiO_2 catalyst. Abbreviations of S, M, and I mean support, metal, and metal-support interface, respectively. Reprinted from Ref. [41].

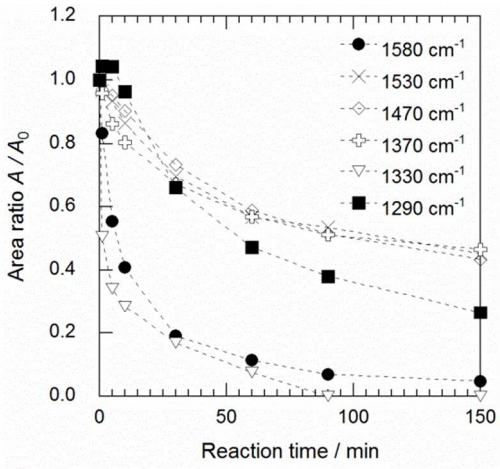

Fig. 4 Decrease in FTIR peak area ratio to the initial peak area at the respective wavenumbers under 5% H_2/Ar flow at 200°C as a function of reaction time. These data were recorded after a switch from the model gas mixture (CO_2/H_2 = 1/9) to 5% H_2/Ar. Catalyst: 2%Ru/CeO_2. Reprinted from Ref. [49]

Based on computational chemistry, debates still exist on the intermediate of CO_2 conversion to CO. Computational chemistry predicted the following three intermediates: formate species (HCOO), [51-53] hydrocarboxyl species (HOCO), [54, 55] and no intermediate (CO dissociation).[53] According to experimental observations, moreover, formate species seem to hardly react with H_2 on reported catalysts with low CO_2 methanation activity, such as Ru/Al_2O_3,[12, 49] Ru/zeolite,[12] and Ni-Al oxides.[45] On the other hand, formate species on Ru/TiO_2 [41, 48, 56] and $Ru/CeO_2/Al_2O_3$ [49] disappeared in H_2 flow. Marwood and coauthors investigated and suggested the mechanism of CO_2

methanation using DRIFT techniques, as shown in Scheme 1. [41] A pathway involving hydrogen carbonate (HCO_3^-) is presented for the formation of the formate species ($HCOO^-$). The formate species adsorbed at the interface between metal and support is expected to be decomposed to H_2 and hydroxyl groups. As for Ru/CeO_2 we attempted to compare the hydrogenation rate of carbonate and formate species.[49] These species were observed as the peaks at 1580, 1530, 1470, 1370, 1330, and 1290 cm^{-1} in the FTIR spectra. The peak areas after desired time of reaction with H_2/Ar were defined as A, and the initial areas as A_0. Fig. 4 shows the peak area ratios (A/A_0) as a function of time-on-stream after switching to H_2/Ar. The bands at 1580 and 1330 cm^{-1} rapidly decreased at an identical rate, and are derived from disappearance of bidentate carbonate species on CeO_2.[57, 58] Interestingly, the three curves for A/A_0 at 1530, 1470, and 1370 cm^{-1} were nearly coincident: the ratios of 1530, 1470, and 1370 cm^{-1} decreased from 1 to ca. 0.6 in 60 min, and then remains. The peaks at 1530, and 1370 cm^{-1} are ascribed to O-C-O asymmetric vibration and C-H in-plane bending vibration in formate species, respectively, while the band at 1470 cm^{-1} are assigned to monodentate carbonate.[57] The ratio drops indicate that a part of formate still remained without reacting with H_2 or being desorbed from the catalyst. Furthermore, thermal stability of the carbonate and formate was also investigated. Under N_2 atmosphere the carbonate peaks (1580 and 1330 cm^{-1}) gradually disappeared, while the formate peaks (1540 and 1390 cm^{-1}) were unchanged. Thus, what follows these results are: (i) the carbonate and a part of the formate species react with H_2, (ii) the carbonate species on Ru/CeO_2 are decomposed or desorbed at high temperature such as 200 ºC, and (iii) the formate species on Ru/CeO_2 are thermally stable at 200 ºC.

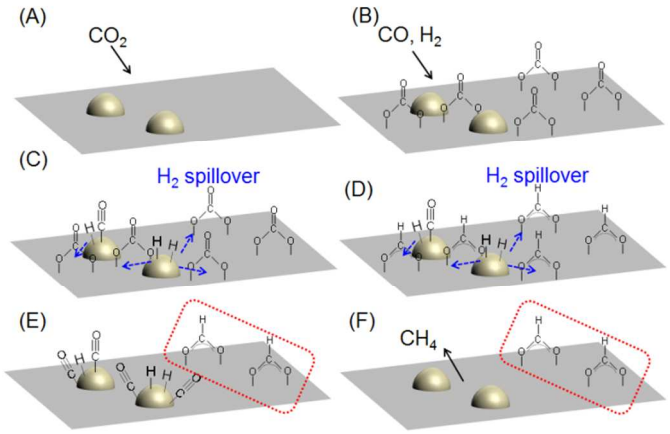

Scheme 2 Plausible mechanism of CO_2 methanation over supported metal catalysts under CO and CO_2 coexisting condition.

Thus we would like to suggest a reaction scheme, as shown in Scheme 2. Firstly CO_2 absorbs on a support material, leading to carbonate species on the support material (Scheme 2 (B)). In addition, CO and H_2 adsorb on an active metal surface (Scheme 2 (C)). Next the hydrogen spillover from the metal enables the carbonate conversion to formate species (Scheme 2 (D)). It is also reported that the carbonate species should react with gas-phase H_2, leading to formate formation.[41] After that, only the formate species in contiguity with the metal are decomposed to CO along the metal-support interface, and the residual (as indicated by a dotted square) are not (Scheme 2 (E)). Finally, the CO adsorbed on metal reacts with H_2 to CH_4 (Scheme 2 (F)). This scheme can explain the following phenomena as discussed above: (i) Gas-phase CO adsorbed on the active metal whose surface was partly occupied CO formed via CO_2 decomposition, and (ii) a part of formate species remain without reaction.

3. Particle size effect

As for selective CO methanation, the catalytic performance of heterogeneous catalysts is expected to depend on the size of active species. This is because basically hydrogenation reaction of CO_x is known to be structure-sensitive. Based on density functional theory (DFT) calculation, dissociation of CO, known as a dominant step of CO methanation, takes place at step-edge sites of metallic Ru, [59-61] Rh, [61, 62] and Ni.[61, 63] On the other hand, Kowalczyk et al. suggested that the turnover frequency of CO hydrogenation was enhanced over Ru catalysts as the Ru dispersion incresed.[64] Therefore these studies seem to predict the optimum metal particle size for CO methanation. The CO_x hydrogenation mechanism on heterogeneous catalysts has been still debated, and no consensus on the particle size effect has been reached,[37, 43, 65, 66] since the effect seems to depend on reaction conditions and natures of methanation catalysts.

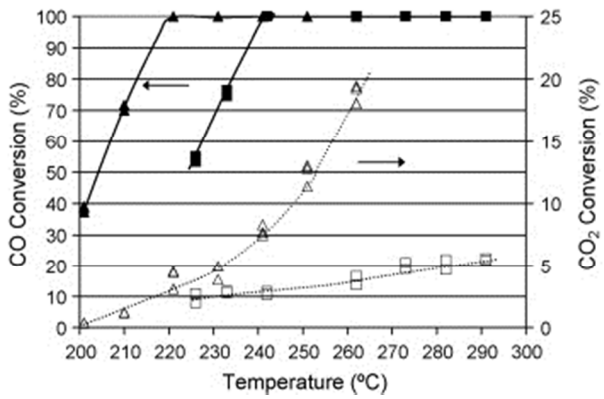

Fig. 5 Effect of crystallite size for a 3% Ru metal loading catalyst on CO and CO2 conversion (feed composition: 0.9% CO, 24.5% CO_2, 68.9% H_2, 5.7% H_2O, SV = 13,500 h^{-1}). Ru crystallite size: (■, multiple-step impregnation) = 34.2 nm, (▲, single-step impregnation) = 10.9 nm. (filled) CO conversion, (open) CO_2 conversion. Reprinted from Ref. [7].

In 2007, the effect of crystallite size of active metal species on selective CO methanation was first reported by Dagle and coauthors.[7] They prepared Ru/Al_2O_3 catalysts by impregnation method, and investigated the effects of loading and crystallite size of Ru and preparation method on the activity and selectivity of CO methanation. The Ru nanoparticles grew due to multicycle impregnation, and an increase in Ru loading amount and pre-reduction temperature by H_2. Fig. 5 illustrates the CO and CO_2 conversion over multi and single-step impregnation $3\%Ru/Al_2O_3$ catalysts. The Ru crystallite size of

the multi and single-step impregnation catalysts were 34.2 and 10.9 nm, respectively. The Ru particle growth shifted the CO and CO_2 conversion curves to higher temperatures, leading to low activity of CO and CO_2 methanation. As an important finding, with growing the Ru particles the activity of CO_2 methanation dropped faster than that of CO methanation. As a result, Ru/Al_2O_3 with larger Ru particles exhibited higher selectivity of CO methanation. The same tendency was also reported by the other studies.[9, 10, 15]

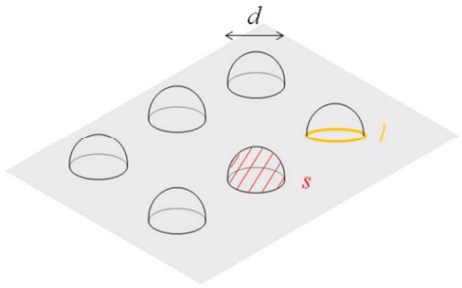

Fig. 6 Hemispherical model of metal particles supported on metal oxides.

Herein, we tried to interpret this effect using hemispherical model, as shown in Fig. 6. Firstly it is assumed that metal particles on the supports are hemispherical in uniform volume, density, and particle size. The total length of the metal-support interface L_{tot} and the total metal surface area S_{tot} were estimated from the following equations.

$$L_{tot} = n \times l \quad \text{(eq. 7)}$$

$$S_{tot} = n \times s \quad \text{(eq. 8)}$$

$$l = \pi d \quad \text{(eq. 9)}$$

$$s = \frac{\pi d^2}{2} \quad \text{(eq. 10)}$$

$$n = \frac{w}{v \times \rho} \quad \text{(eq. 11)}$$

$$v = \frac{\pi d^3}{12} \quad \text{(eq. 12)}$$

where n is the number of particles per unit mass of catalyst, l is the perimeter of a particle, s is the metal surface area of a particle, d is the particle size of the metal, w is the loading amount, v is the volume of the metal, and ρ is the density of the metal. According to these equations, L_{tot} and S_{tot} should be proportional to d^{-2} and d^{-1}, respectively, indicating that the particle growth strongly affects the diminution of L_{tot} compared to the decrease of S_{tot}. Thus the activity of CO_2 methanation can decrease faster than that of CO methanation if CO and CO_2 methanation take place at the metal surface and along the metal-support interface, respectively. This assumption interestingly agrees with the Dagle's experimental data as mentioned above, and can inform the importance of controlling the metal-support interface in order to prepare a suitable catalyst with high CO methanation selectivity.

4. Enhancement of CO methanation activity

Achievement of complete CO removal at low temperature can avoid exothermic CO_2 methanation at high temperatures. As a simple solution, an increase in the amount of exposed active species can enhance the CO methanation activity. Indeed, adding of noble metal (such as Ru, [67, 68] and Pt [69]) to Ni-containing mixed oxide catalysts boosted CO methanation at low temperature because H_2 spillover from the noble metal enhanced the reducibility of the Ni species, as will be seen in section 5.1. The other answer is the control of CO adsorption and dissociation, since the adsorption and dissociation at an active metal surface are key steps for CO methanation. It is considered that the electron density (ED) of the surface directly influences on the activity of CO methanation. If the ED is enhanced, CO adsorbed on a metal surface with high ED is more easily dissociated by enhanced $d\pi$-$p\pi^*$ back bonding and consequently CO methanation is improved.[33, 70, 71] Otherwise, the amount of dissociatively-adsorbed H_2 on the metal increases due to weak adsorption of CO on the surface, which favors the transformation of CO to CH_4.[42] These investigations show the importance of finding the suitable ED for selective CO methanation. Basically the ED can be changed by the following processes: (i) change of a support material,[72] and (ii) addition of some promoters, such as alkali and alkali earth metal, to catalysts.[73-77] In this section, we summarized them.

4.1 Role of support material

As for Ru catalyst, the activity for CO hydrogenation was significantly improved when Ru nanoparticles were supported on TiO_2 compared to Al_2O_3, CeO_2, YSZ, SiO_2, ZrO_2, and MgO, under CO,[4, 78] and CO-CO_2 coexisting condition.[8, 9, 15] According to the XANES and EXAFS data reported by Takenaka and coauthors, the nature of support material did not affect the oxidation state of Ru NPs, while did that of Ni species.[4] Compared to Ni/ZrO_2, Ni/TiO_2, and Ni/SiO_2, the Ni species on Ni/Al_2O_3 and Ni/MgO were partly oxidized and showed the low activity of CO hydrogenation. Regrettably, there are almost no reports about the relationship between the support nature and the ED of active metal in the selective CO methanation field. In the studies introduced above, the size of active metals depended on the nature of support materials, which affected the CO methanation activity.

4.2 Role of Promoter

Under CO and CO_2 coexisting condition, interestingly, K [6] and Na [10] residual on the Ru/TiO_2 catalyst surface decreased the apparent activity of CO methanation, while addition of La species [6] to Ru/TiO_2 improved the apparent activity. In addition, these three promoters enhanced the activity of CO_2

methanation.[6, 10] Thus the Ru-La/TiO_2 catalyst appears to be succeeding in CO removal at lower temperature than the unmodified Ru/TiO_2 catalyst. The XPS peak positions attributed to Ru $d_{5/2}$ orbital on Ru/TiO_2, Ru-La/TiO_2, and Ru-K/TiO_2 were at 280.5, 280.2, and 280.1 eV, respectively, indicating of enhancement of the ED of Ru species by La and K addition to Ru/TiO_2. From the XPS results, the La and K additives were expected to exist beside Ru species, which enhances CH_4 production rate from carbon monoxide. Carbon dioxide is known to be adsorbed on La_2O_3 and K_2O to form lanthanum and potassium carbonates with high thermal stability.[79, 80] It is also reported that the addition of Na species to Ru catalysts enhanced CO_2 methanation due to a large amount of CO_2 chemisorption. [81] Therefore it is likely that the La, K, and Na additives can function as CO_2 supply sources, leading to improvement of CO production via RWGS reaction. Similar mechanism was reported by Park et al. in CO_2 methanation over Pd-MgO/SiO_2: palladium metal provides atomic hydrogen to magnesium carbonate to form methane, and then the methane is desorbed, followed by magnesium carbonate reproduction via the adsorption of gas phase CO_2 on magnesium oxides produced in the reaction.[44] If the La, K, and Na species play a role similar to MgO on Pd-MgO/SiO_2, Ru-K/TiO_2 and Ru-La/TiO_2, Ru-K/TiO_2, and Ru-Na/TiO_2 can also boost RWGS reaction and CO_2 methanation. As for Ru-K/TiO_2 and Ru-Na/TiO_2, CO production rate by RWGS reaction is probably higher than CO consumption rate by methanation, giving rise to slower decrease in CO concentration.

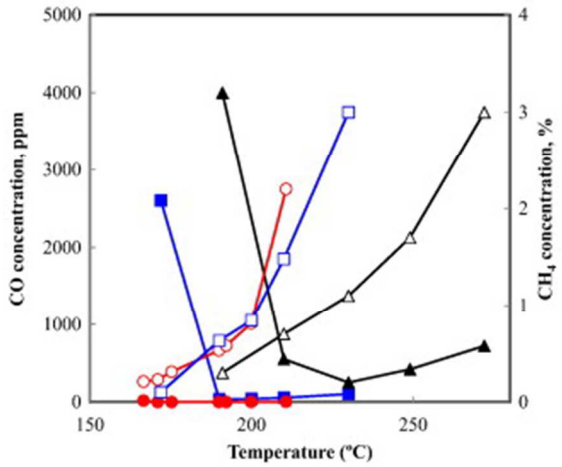

Fig. 7 Temperature dependence for selective CO methanation over Ni/Al_2O_3 (triangles), $Ni/AlVO_x$ (squares), and mesoporous SiO_2-TiO_2 coated $Ni/AlVO_x$ (circles). (filled) CO concentration, (open) CH_4 concentration. Reaction conditions: $CO/CO_2/H_2/H_2O$ = 0.43/17.1/67.9/14.5, GHSV = 2400 h^{-1}. Reproduced from Ref. [82].

Vanadium oxide is also known as a promoter for CO methanation. Mori et al. expected that V^{3+} ions in the vicinity of active metal extracts an oxygen atom in hydroxycarbene (-CHOH), leading to easy dissociation of CO.[83] Recently $Ni/AlVO_x$ [82] and Ni-V_2O_3/Al_2O_3 [84] catalysts was reported, and showed the higher activity of CO and CO_2 methanation than Ni/Al_2O_3. Therefore vanadium promoter does not seem suitable for selective CO methanation. In order to suppress only the CO_2 methanation activity, Miyao et al. covered the surface of $Ni/AlVO_x$ with a mesoporous SiO_2-TiO_2 layer. [82] Fig. 7 shows the CO and CH_4 concentration over Ni/Al_2O_3, $Ni/AlVO_x$, and mesoporous SiO_2-TiO_2 coated $Ni/AlVO_x$ catalysts. The coating did not change the CH_4 formation at high temperature compared to $Ni/AlVO_x$, while the coated catalysts eliminated CO much more than uncoated catalysts. According to these results, the coated catalysts exhibited high activity and selectivity of CO methanation at low temperature.

5. Suppression of CO_2 adsorption and/or CO_2 conversion

According to reaction mechanism of CO_2 methanation (section 2.2) and promoter effect (section 4), CO_2 adsorption on catalysts and CO_2 conversion to CO are key steps of CO_2 methanation. Actually, several researchers reported that CO_2 methanation activity is enhanced with an increase in the CO_2 adsorption.[29, 44, 49, 50] In other words, it should be of little surprise that suppression of the CO_2 adsorption hinders CO_2 methanation. Under the CO and CO_2 coexisting condition, CO_2 methanation over Ru/TiO_2 was suppressed in spite of long perimeter compared to Ru/Al_2O_3, stemming from the small amount of CO_2 adsorbed onto Ru/TiO_2.[9]

5.1 Ru-Ni bimetallic catalyst

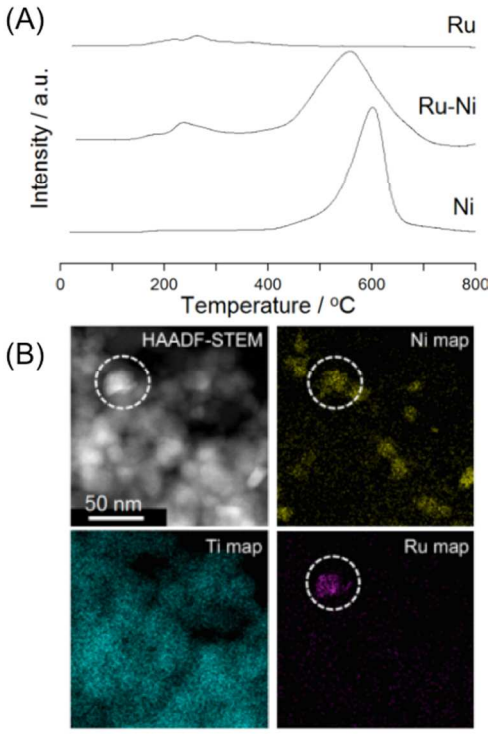

Fig. 8 (A) H_2-TPR profiles of 0.5wt%Ru/TiO_2, 0.5wt%Ru-5wt%Ni/TiO_2, and 5wt%Ni/TiO_2. (heating rate = 10ºC/min). Reproduced from Ref. [48]. (B) STEM-HAADF image and Ti, Ni, and Ru maps of 0.5wt%Ru-5wt%Ni/TiO_2. Reproduced from Ref. [85].

Bimetallic Ru-Ni/TiO_2 catalyst was developed as an answer to shortening of the perimeter between Ru and TiO_2. [48] In order to determine the geometric character of Ru and Ni species on the catalyst, temperature programmed reduction by H_2 (H_2-TPR, Fig. 8(A)) was firstly conducted. The peaks at ca. 220 and 550ºC were attributed to reduction of RuO_2 and NiO. It is noteworthy that the loading amounts of Ru and Ni determined by H_2-TPR are close to those measured by ICP-AES, which means that Ru species existed without forming solid solution with the Ni species. In addition, the reduction peak of NiO was shifted to lower temperature by adding Ru to Ni/TiO_2, indicating of enhancement of Ni reducibility due to H_2 spillover from metallic Ru to NiO. The reduction of NiO by the spillover H_2 requires close contact of Ni species with Ru metal. These considerations were backed by scanning transmission electron microscopy (STEM) images and EDS maps, as shown in Fig. 8 (B): Ru and Ni signals on the EDS maps (in the dotted circle) were overlapped.[85] Thus the combination of Ru and Ni species on the Ru-Ni/TiO_2 catalysts was expected to decrease in direct contact between Ru and TiO_2. This Ru-Ni catalyst exhibited higher CO methanation activity and lower CO_2 methanation activity than Ru/TiO_2. Briefly, this was because the decomposition of formate species, known as a CO_2 methanation intermediate, on Ru-Ni/TiO_2 was suppressed compared to Ru/TiO_2.[48]

Chen et al. have reported the effect of loading amount of Ru (0 or 1wt%) and Ni (0, 10, 20, 33, 40, 50 wt%) on catalytic performance of selective CO methanation using Ru/mesoporous Ni-Al oxides.[68] The catalytic activity and selectivity of CO methanation was enhanced by (i) increasing Ni content in the Ru/ mesoporous Ni-Al oxides and (ii) adding Ru to the mesoporous Ni-Al oxides. They focused on the specific surface area (SSA) difference of the catalysts between with and without Ru: the SSA was dramatically increased by the addition of Ru species to reduced mesoporous Ni-Al oxides. This is because the H_2 spillover from Ru species boosted the NiO reduction. Therefore it is expected that the Ru addition increased the amount of exposed metallic Ni on mesoporous Ni-Al oxides, leading to high CO methanation activity over Ru/mesoporous Ni-Al oxides. Furthermore they considered that the Ru inclusion to Ni-Al oxides hindered the CO_2 dissociation to CO, resulting in high selectivity of CO methanation.[67] The hindrance seems to be influenced by not only the combination of Ru and Ni but also existence of chlorine (as will be seen in section 5.2) since they used $RuCl_3{\cdot}xH_2O$ as a Ru precursor.

5.2 Chlorine modification

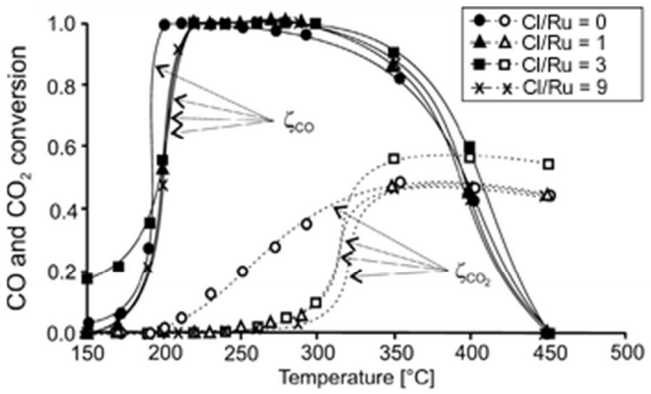

Fig. 9 Effect of impregnation of NH_4Cl solution to 1%Ru/Al_2O_3 catalyst synthesized with Ru(NO)$(NO_3)_3$ precursor on CO and CO_2 conversion. Three different chlorine molar loads (Cl/Ru = 1, 3, and 9) were added to the 1%Ru/Al_2O_3 (Cl/Ru = 0). (filled) CO conversion, (open) CO_2 conversion. Reaction condition: $CO/CO_2/H_2/N_2$ = 0.5/18/40/41, space velocity = 0.33 NL min^{-1} g_{cat}^{-1}.Reproduced from Ref. [25].

It is reported that modification of methanation catalysts by chlorine component suppresses CO_2 adsorption and/or CO_2 dissociation to CO, resulting in high selectivity of CO methanation. Using Ru/Al_2O_3 catalysts prepared by incipient wetness impregnation, Djinovic and coauthors attempted to clarify the effect of Ru precursors ($RuCl_3{\cdot}xH_2O$ and Ru(NO)$(NO_3)_3$) [24, 25] and presence of chlorine on selective CO methanation.[25] The catalyst prepared from $RuCl_3{\cdot}xH_2O$ had low activities of CO and CO_2 methanation compared to that from Ru(NO)$(NO_3)_3$. It is important to note that the chlorine-containing catalyst exhibited higher selectivity of CO methanation than chlorine-free one, due to strong suppression of CO_2 methanation. In addition, impregnation of Ru/Al_2O_3, prepared from Ru(NO)$(NO_3)_3$, with NH_4Cl solution directly controlled surface chlorine loads on the catalysts, as shown in Fig. 9. As for chlorine-containing catalysts, the lowest temperature where CO conversion is 1 was slightly shifted to higher temperature (10-19ºC) compared to the chlorine-free catalyst. For Ru/Al_2O_3 (Cl/Ru = 0), CO_2 conversion gradually rose from 200ºC to 350ºC, and then was steady at ca. 50%. Over the Ru/Al_2O_3 with chlorine components, the conversion remained ca. 0% below 250ºC, and then started to increase rapidly. According to these results, chlorine modification of Ru/Al_2O_3 succeeded to enhance the selectivity of CO methanation as well. Miyao et al. pointed from the result of temperature programmed desorption of CO_2 that CO_2 hardly adsorbed on chlorine-containing catalysts.[45] Moreover it was concluded that chlorine components were located on Ni surface. This is because CO methanation proceeding on Ni surface was suppressed by chlorine modification. Zyryanova et al. adjusted the surface chlorine amount on Ni/CeO_2 catalysts using nickel salt mixture at various ratios of $NiCl_2$ and $Ni(NO_3)_2$.[86] The higher the chlorine content is, the lower the methanation activity of CO and CO_2 was. Based on the other works, [87, 88] high reduction of the Ni/CeO_2 was expected to form stable $Ce^{3+}OCl$ surface species, probably leading to the interference of CO_2 adsorption and/or CO_2 dissociation.

6. Conclusions and perspective

Based on the mechanistic studies for selective CO methanation (Scheme 2), we suggest that the key of selective CO methanation is the control of interfaces between active metals and support materials (section 3). If the interface can be blocked or the perimeter can be shortened, CO_2 conversion to CO will be hindered, leading to high CO methanation selectivity. As mentioned in section 5, the following solutions can prove quite effective in enhancement of CO methanation selectivity: (i) the combination of Ru and Ni, and (ii) chlorine modification. In addition, it can be necessary to choose suitable support materials and promoters, otherwise undesirable CO_2 methanation will proceed (section 4).

At the present stage developed Ru and/or Ni catalysts is approaching the practical use. In order to put into practical use, sophisticated catalysts with high stability (more than 40,000 h) [89] and high activity should be developed. Long-term tests for selective CO methanation over the developed catalysts have recently been conducted, as summarized in Table 1. A plenty number of developed catalysts show the great activity of CO methanation, while they need stability improvement because they had work for less than 10,000 h. Thus it is expected that clarification of deactivation mechanism for selective CO methanation catalysts is next on our challenge, which will allow the development of new suitable catalysts with high activity and selectivity of CO methanation.

In order to decrease fossil fuel consumption and harmful influence on the global environment, it is important to develop new technologies for effective utilization of fossil fuels. As one of the technologies, we focus on polymer electrolyte fuel cell (PEFC) systems with high power density and high total energy conversion efficiency. Developing selective CO methanation catalysts and alternating from the unit of preferential oxidation of CO (PROX) to that of selective CO methanation will lead to a decline in manufacture's cost of PEFC systems, resulting in spreading installation sites of PEFC.

Notes and references

[a] Department of Chemical System Engineering, School of Engineering, The University of Tokyo, 7-3-1 Hongo, Bunkyo-ku, Tokyo 113-8656, Japan.
[b] Japan Society for the Promotion of Science, 5-3-1 Kojimachi, Chiyoda-ku, Tokyo 102-0083, Japan.
[c] Present address: Department of Chemistry and Applied Biosciences, ETH Zürich, Vladmir-Prelog-Weg 2, Zürich CH-8093, Switzerland.

Shohei Tada is currently a postdoctoral fellow in the group of Prof. Ryuji Kikuchi and Prof. S. Ted Oyama at the University of Tokyo. He received his BE, ME, and PhD degrees from the University of Tokyo, supervised by Prof. Ryuji Kikuchi. He is a JSPS research fellow for young scientists from 2013, and a guest researcher at ETH Zürich from 2014. His research focuses on conversion of CO and CO_2 to chemicals.

Table 1 Long-term test for selective CO methanation.

Catalysts	Reaction Temp./ ºC	Reaction Time/ h	Space velocity	CO conc. / ppm	Composition					Ref.
					CO	CO_2	H_2	H_2O	Inert	
5%Ru/TiO_2	220	10	0.20 g_{cat} min L^{-1}*	< 30	0.5	15	60	0.9	24.9 (He)	[4]
0.5%Ru-10%Ni/TiO_2	200	5500	10000 h^{-1}	< 100	0.2	16.1	65.3	18.4		[90]
10%Ni/TiO_2	200	7000	2500 h^{-1}	< 100	0.2	16.1	65.3	18.4		[90]
5%Ni/m-ZrO_2	240	140	10000 h^{-1}	< 10	0.425	17	63.325	15	4.25 (N_2)	[27]
1%Ru/Ni-Al oxide	200	200	2800 h^{-1}	< 10	0.85	17	67.15	15		[68]
Mesoporous SiO_2-TiO_2 coated Ni/$AlVO_x$	193	> 4000	2400 h^{-1}	-	0.43	17.1	67.9	14.5		[82]
7%Ru-ZrO_2/ CNTs-Ni	200	36	1000 h^{-1}	< 10	1	20	79			[91]
2%Ru/Al_2O_3	320	72	3000 h^{-1}	-	25		75			[20]
5%Ru/TiO_2	230	90	49000 h^{-1}	-	0.5	15	55.5	30		[15]
43%Ni/Cr_2O_3/Al_2O_3	300	180	0.42 g_{cat} min L^{-1}*	< 50	1.6	12.5	37.5	25	23.4 (N_2)	[92]

* W/F

Ryuji Kikuchi is an Associate Professor in the Department of Chemical System Engineering at the University of Tokyo. He received his BE, ME, and PhD degrees from the University of Tokyo. He was a postdoctoral fellow at ETH Zürich from 1997 to 1998, a postdoctoral fellow at the University of Tokyo from 1998 to 2000, a research associate at Kyushu University from 2000 to 2001, a research associate and an Associate Professor at Kyoto University from 2001 to 2008, and an Associate Professor at the University of Tokyo from 2008. His research focuses on reforming of hydrocarbons, fuel cells, and electrochemical synthesis of chemicals.

1. I. Staffell and R. Green, *Int J Hydrogen Energ*, 2013, **38**, 1088.
2. E. Antolini, *J Appl Electrochem*, 2004, **34**, 563.
3. P. Panagiotopoulou, D. I. Kondarides and X. E. Verykios, *Appl Catal A: Gen*, 2008, **344**, 45.
4. S. Takenaka, T. Shimizu and K. Otsuka, *Int J Hydrogen Energ*, 2004, **29**, 1065.
5. K. Urasaki, Y. Tanpo, T. Takahiro, J. Christopher, R. Kikuchi, T. Kojima and S. Satokawa, *Chem Lett*, 2010, **39**, 972.
6. S. Tada, R. Kikuchi, A. Takagaki, T. Sugawara, S. Ted Oyama and S. Satokawa, *Catal Today*, 2014, **232**, 16.
7. R. A. Dagle, Y. Wang, G. G. Xia, J. J. Strohm, J. Holladay and D. R. Palo, *Appl Catal A: Gen*, 2007, **326**, 213.
8. K. Urasaki, K. Endo, T. Takahiro, R. Kikuchi, T. Kojima and S. Satokawa, *Top Catal*, 2010, **53**, 707.
9. S. Tada, R. Kikuchi, K. Urasaki and S. Satokawa, *Appl Catal A: Gen*, 2011, **404**, 149.
10. S. Tada and R. Kikuchi, *Catal Sci Technol*, 2014, **4**, 26.
11. S. Eckle, H. G. Anfang and R. J. Behm, *Appl Catal A: Gen*, 2011, **391**, 325.
12. S. Eckle, H. G. Anfang and R. J. Behm, *J Phys Chem C*, 2011, **115**, 1361.
13. S. Eckle, M. Augustin, H. G. Anfang and R. J. Behm, *Catal Today*, 2012, **181**, 40.
14. S. Eckle, Y. Denkwitz and R. J. Behm, *J Catal*, 2010, **269**, 255.
15. P. Panagiotopoulou, D. I. Kondarides and X. E. Verykios, *Appl Catal B: Environ*, 2009, **88**, 470.
16. P. Panagiotopoulou, D. I. Kondarides and X. E. Verykios, *J Phys Chem C*, 2011, **115**, 1220.
17. P. Panagiotopoulou, D. I. Kondarides and X. E. Verykios, *Catal Today*, 2012, **181**, 138.
18. V. Jimenez, P. Sanchez, P. Panagiotopoulou, J. L. Valverde and A. Romero, *Appl Catal A: Gen*, 2010, **390**, 35.
19. O. Gorke, P. Pfeifer and K. Schubert, *Catal Today*, 2005, **110**, 132.
20. Y. F. Zhang, G. J. Zhang, L. P. Wang, Y. Xu and Y. L. Sun, *J Ind Eng Chem*, 2012, **18**, 1590.
21. C. Galletti, S. Specchia, G. Saracco and V. Specchia, *Chem Eng Sci*, 2010, **65**, 590.
22. C. Galletti, S. Specchia and V. Specchia, *Chem Eng J*, 2011, **167**, 616.
23. X. H. Lin, K. Yang, R. R. Si, X. Chen, W. X. Dai and X. Z. Fu, *Appl Catal B: Environ*, 2014, **147**, 585.
24. P. Djinovic, C. Galletti, S. Specchia and V. Specchia, *Catal Today*, 2011, **164**, 282.
25. P. Djinovic, C. Galletti, S. Specchia and V. Specchia, *Top Catal*, 2011, **54**, 1042.
26. K. Urasaki, Y. Tanpo, Y. Nagashima, R. Kikuchi and S. Satokawa, *Appl Catal A: Gen*, 2013, **452**, 174.
27. A. Chen, T. Miyao, K. Higashiyama and M. Watanabe, *Catal Sci Technol*, 2014, **4**, 2508.
28. X. Z. Yang, X. Wang, G. J. Gao, Wendurima, E. M. Liu, Q. Q. Shi, J. N. Zhang, C. H. Han, J. Wang, H. L. Lu, J. Liu and M. Tong, *Int J Hydrogen Energ*, 2013, **38**, 13926.
29. D. C. D. da Silva, S. Letichevsky, L. E. P. Borges and L. G. Appel, *Int J Hydrogen Energ*, 2012, **37**, 8923.
30. E. D. Park, D. Lee and H. C. Lee, *Catal Today*, 2009, **139**, 280.
31. P. Panagiotopoulou, D. I. Kondarides and X. E. Verykios, *Ind Eng Chem Res*, 2011, **50**, 523.
32. G. Kolb, *Chem Eng Process*, 2013, **65**, 1.
33. F. Solymosi, I. Tombacz and M. Kocsis, *J Catal*, 1982, **75**, 78.
34. M. Araki and V. Ponec, *J Catal*, 1976, **44**, 439.
35. J. Kopyscinski, T. J. Schildhauer, F. Vogel, S. M. A. Biollaz and A. Wokaun, *J Catal*, 2010, **271**, 262.
36. N. M. Gupta, V. S. Kamble, V. B. Kartha, R. M. Iyer, K. R. Thampi and M. Gratzel, *J Catal*, 1994, **146**, 173.
37. F. Ocampo, B. Louis and A. C. Roger, *Appl Catal A: Gen*, 2009, **369**, 90.
38. A. E. Aksoylu and Z. I. Onsan, *Appl Catal A-Gen*, 1997, **164**, 1.
39. D. E. Peebles, D. W. Goodman and J. M. White, *J Phys Chem*, 1983, **87**, 4378.
40. M. Yamasaki, H. Habazaki, K. Asami, K. Izumiya and K. Hashimoto, *Catal Commun*, 2006, **7**, 24.
41. M. Marwood, R. Doepper and A. Renken, *Appl Catal A: Gen*, 1997, **151**, 223.
42. S. Scire, C. Crisafulli, R. Maggiore, S. Minico and S. Galvagno, *Catal Lett*, 1998, **51**, 41.
43. A. Karelovic and P. Ruiz, *Appl Catal B: Environ*, 2012, **113**, 237.
44. J. N. Park and E. W. McFarland, *J Catal*, 2009, **266**, 92.
45. T. Miyao, W. Shen, A. Chen, K. Higashiyama and M. Watanabe, *Appl Catal A: Gen*, 2014, **486**, 187.
46. S. Y. Chin, C. T. Williams and M. D. Amiridis, *J Phys Chem B*, 2006, **110**, 871.
47. S. M. Vesecky, X. P. Xu and D. W. Goodman, *J Vac Sci Technol A*, 1994, **12**, 2114.
48. S. Tada, R. Kikuchi, A. Takagaki, T. Sugawara, S. T. Oyarria, K. Urasaki and S. Satokawa, *Appl Catal B: Environ*, 2013, **140 - 141**, 258.

49. S. Tada, O. J. Ochieng, R. Kikuchi, T. Haneda and H. Kameyama, *Int J Hydrogen Energ*, 2014, **39**, 10090.
50. S. Tada, T. Shimizu, H. Kameyama, T. Haneda and R. Kikuchi, *Int J Hydrogen Energ*, 2012, **37**, 5527.
51. R. J. Madon, D. Braden, S. Kandoi, P. Nagel, M. Mavrikakis and J. A. Dumesic, *J Catal*, 2011, **281**, 1.
52. R. G. Zhang, B. J. Wang, H. Y. Liu and L. X. Ling, *J Phys Chem C*, 2011, **115**, 19811.
53. S. Akamaru, T. Shimazaki, M. Kubo and T. Abe, *Appl Catal A: Gen*, 2014, **470**, 405.
54. E. Vesselli, M. Rizzi, L. De Rogatis, X. L. Ding, A. Baraldi, G. Comelli, L. Savio, L. Vattuone, M. Rocca, P. Fornasiero, A. Baldereschi and M. Peressi, *J Phys Chem Lett*, 2010, **1**, 402.
55. A. A. Gokhale, J. A. Dumesic and M. Mavrikakis, *J Am Chem Soc*, 2008, **130**, 1402.
56. M. R. Prairie, A. Renken, J. G. Highfield, K. R. Thampi and M. Gratzel, *J Catal*, 1991, **129**, 130.
57. C. Li, Y. Sakata, T. Arai, K. Domen, K. I. Maruya and T. Onishi, *J Chem Soc Faraday Trans 1*, 1989, **85**, 1451.
58. G. Busca, J. Lamotte, J. C. Lavalley and V. Lorenzelli, *J Am Chem Soc*, 1987, **109**, 5197.
59. R. A. Van Santen, *Acc Chem Res*, 2009, **42**, 57.
60. I. M. Ciobica and R. A. van Santen, *J Phys Chem B*, 2003, **107**, 3808.
61. A. C. Lausche, A. J. Medford, T. S. Khan, Y. Xu, T. Bligaard, F. Abild-Pedersen, J. K. Norskov and F. Studt, *J Catal*, 2013, **307**, 275.
62. M. Mavrikakis, M. Baumer, H. J. Freund and J. K. Norskov, *Catal Lett*, 2002, **81**, 153.
63. M. P. Andersson, E. Abild-Pedersen, I. N. Remediakis, T. Bligaard, G. Jones, J. Engbwk, O. Lytken, S. Horch, J. H. Nielsen, J. Sehested, J. R. Rostrup-Nielsen, J. K. Norskov and I. Chorkendorff, *J Catal*, 2008, **255**, 6.
64. Z. Kowalczyk, K. Stolecki, W. Rarog-Pilecka, E. Miskiewicz, E. Wilczkowska and Z. Karpiniski, *Appl Catal A: Gen*, 2008, **342**, 35.
65. T. Abe, M. Tanizawa, K. Watanabe and A. Taguchi, *Energy Environ Sci*, 2009, **2**, 315.
66. C. S. Kellner and A. T. Bell, *J Catal*, 1982, **75**, 251.
67. M. Kimura, T. Miyao, S. Komori, A. H. Chen, K. Higashiyama, H. Yamashita and M. Watanabe, *Appl Catal A: Gen*, 2010, **379**, 182.
68. A. Chen, T. Miyao, K. Higashiyama, H. Yamashita and M. Watanabe, *Angew Chem Int Ed*, 2010, **49**, 9895.
69. H. Yoshida, K. Watanabe, N. Iwasa, S.-I. Fujita and M. Arai, *Appl Catal B: Environ*, 2015, **162**, 93.
70. T. Ishihara, K. Harada, K. Eguchi and H. Arai, *J Catal*, 1992, **136**, 161.
71. T. Iizuka, Y. Tanaka and K. Tanabe, *J Catal*, 1982, **76**, 1.
72. A. G. T. M. Bastein, W. J. Vanderboogert, G. Vanderlee, H. Luo, B. Schuller and V. Ponec, *Appl Catal*, 1987, **29**, 243.
73. S. T. Hussain, M. A. Nadeem and M. Mazhar, *Catal Commun*, 2008, **9**, 2048.
74. Z. C. Tao, Y. Yang, M. G. Ding, T. Z. Li, H. W. Xiang and Y. W. Li, *Catal Lett*, 2007, **117**, 130.
75. Y. Okamoto, E. Matsunaga, T. Imanaka and S. Teranishi, *J Catal*, 1982, **74**, 183.
76. K. Murata, K. Okabe, M. Inaba, I. Takahara and Y. Y. Liu, *Catal Lett*, 2009, **128**, 343.
77. R. D. Gonzalez and H. Miura, *J Catal*, 1982, **77**, 338.
78. Y. H. Kim, E. D. Park, H. C. Lee and D. Lee, *Appl Catal A: Gen*, 2009, **366**, 363.
79. A. N. Shirsat, M. Ali, K. N. G. Kaimal, S. R. Bharadwaj and D. Das, *Thermochim Acta*, 2003, **399**, 167.
80. C. S. Chen, W. H. Cheng and S. S. Lin, *Appl Catal A: Gen*, 2003, **238**, 55.
81. D. Theleritis, M. Makri, S. Souentie, A. Caravaca, A. Katsaounis and C. G. Vayenas, *ChemElectroChem*, 2014, **1**, 254.
82. T. Miyao, S. Sakurabayashi, W. Shen, K. Higashiyama and M. Watanabe, *Catal Commun*, 2015, **58**, 93.
83. T. Mori, A. Miyamoto, N. Takahashi, M. Fukagaya, T. Hattori and Y. Murakami, *J Phys Chem*, 1986, **90**, 5197.
84. Q. Liu, F. Gu, X. Lu, Y. Liu, H. Li, Z. Zhong, G. Xu and F. Su, *Appl Catal A: Gen*, 2014, **488**, 37.
85. S. Tada, D. Minori, F. Otsuka, R. Kikuchi, K. Osada, K. Akiyama and S. Satokawa, *Fuel*, 2014, **129**, 219.
86. M. M. Zyryanova, P. V. Snytnikov, R. V. Gulyaev, Y. I. Amosov, A. I. Boronin and V. A. Sobyanin, *Chem Eng J*, 2014, **238**, 189.
87. L. Kepiński, M. Wolcyrz and J. Okal, *J Chem Soc Faraday Trans*, 1995, **91**, 507.
88. F. Le Normand, J. Barrault, R. Breault, L. Hilaire and A. Kiennemann, *J Phys Chem*, 1991, **95**, 257.
89. Hydrogen, Fuel Cells & Infrastructure Thechnologies Program, *Technical Plan*, Multi-Year Research, Development and Demonstration Plan, U. S. DOE, Washington, 2007.
90. S. Tada, R. Kikuchi, K. Wada, K. Osada, K. Akiyama, S. Satokawa and Y. Kawashima, *J Power Sources*, 2014, **264**, 59.
91. J. Xiong, X. F. Dong, Y. B. Song and Y. C. Dong, *J Power Sources*, 2013, **242**, 132.
92. Y. Men, G. Kolb, R. Zapf, M. O'Connell and V. Hessell, *Chem Lett*, 2009, **38**, 824.

Table of Contents

As for selective CO methanation over heterogeneous catalysts, the numerous investigations of reaction mechanism and catalyst development are reviewed.